Fractional Laplacian in bounded domains

A. Zoia,[1,2,*] A. Rosso,[1,3] and M. Kardar[1]

[1]*Department of Physics, Massachusetts Institute of Technology, Cambridge, Massachusetts 02139, USA*
[2]*Department of Nuclear Engineering, Polytechnic of Milan, Milan 20133, Italy*
[3]*CNRS—Laboratoire de Physique Théorique et Modéles Statistiques, Université Paris-Sud, F-91405 Orsay Cedex, France*

The fractional Laplacian operator $-(-\Delta)^{\alpha/2}$ appears in a wide class of physical systems, including Lévy flights and stochastic interfaces. In this paper, we provide a discretized version of this operator which is well suited to deal with boundary conditions on a finite interval. The implementation of boundary conditions is justified by appealing to two physical models, namely, hopping particles and elastic springs. The eigenvalues and eigenfunctions in a bounded domain are then obtained numerically for different boundary conditions. Some analytical results concerning the structure of the eigenvalue spectrum are also obtained.

I. INTRODUCTION

Random walks and the associated diffusion equation are at the heart of quantitative descriptions of a large number of physical systems [1,2]. Despite such ubiquity, random walk dynamics has limitations, and does not apply to cases where collective dynamics, extended heterogeneities, and other sources of long-range correlations lead to so-called *anomalous dynamics* [3–5]. To describe these situations, various generalizations of Brownian motion have been conceived, generally covered under the rubric of *fractional dynamics* [3]. For example, a quite useful model of *superdiffusive* behavior, in which the spread of the distribution grows faster than linearly in time, is provided by Lévy flights: particles are assumed to perform random jumps with step lengths taken from a distribution that decays as a power law. If the variance of the jump length is infinite, the central limit theorem does not apply [6–10], and the dynamics is anomalous. Lévy flights, which are dominated by rare but extremely large jumps, have proven quite suitable in modeling many physical systems, ranging from turbulent fluids to contaminant transport in fractured rocks, from chaotic dynamics to disordered quantum ensembles [3,5,11–16].

While the concentration $C(x,t)$ of particles performing Brownian motion follows the standard diffusion equation $\partial_t C(x,t) = \partial_x^2 C(x,t)$, the concentration of particles performing Lévy flights satisfies a *fractional diffusion equation* in which the Laplacian operator is replaced by a *fractional derivative*

$$\frac{\partial}{\partial t}C(x,t) = \frac{\partial^\alpha}{\partial|x|^\alpha}C(x,t). \tag{1}$$

In Eq. (1), $\partial^\alpha/\partial|x|^\alpha$ is the Riesz-Feller derivative of fractional order $\alpha > 0$ [17,18], which has an integral representation involving a singular kernel of power-law form (see Appendix A 1). For diffusing particles, the index α roughly characterizes the degree of fractality of the environment, and is in this context restricted to $\alpha \le 2$; for $\alpha > 2$, the correlations decay

sufficiently fast for the central limit theorem to hold, and Eq. (1) is replaced by the regular diffusion [2].

Interestingly, the same Riesz-Feller derivative also appears in connection with stochastically growing surfaces [19,20]. In this case, the evolution of the height $h(x,t)$ of the interface is usually written in Langevin form

$$\frac{\partial}{\partial t}h(x,t) = \frac{\partial^\alpha}{\partial|x|^\alpha}h(x,t) + \eta(x,t), \tag{2}$$

where $\eta(x,t)$ represents uncorrelated noise of zero mean, and with $\langle \eta(x,t)\eta(x',t')\rangle = 2T\delta(x-x')\delta(t-t')$. The fractional derivative mimics the effects of a generalized elastic restoring force. When $\alpha = 2$, Eq. (2) describes the dynamics of a thermally fluctuating elastic string and is also known as the Edwards-Wilkinson equation [21]. However, in many physical systems, such as crack propagation [22] and the contact lines of a liquid meniscus [23], the restoring forces acting on $h(x,t)$ are long ranged and characterized by $\alpha = 1$. Other physical systems, such as slowly growing films in molecular beam epitaxy, are better described by a restoring force that depends on curvature, with $\alpha = 4$ [24].

Better understanding of the properties of the fractional derivative is thus relevant to many physical systems. When the domain over which the operator $\partial^\alpha/\partial|x|^\alpha$ acts is unbounded, the fractional derivative has a simple definition in terms of its Fourier transform

$$\frac{\partial^\alpha}{\partial|x|^\alpha}e^{iqx} = -|q|^\alpha e^{iqx}. \tag{3}$$

More precisely, $\partial^\alpha/\partial|x|^\alpha$ is an operator whose action on a function $F(x)$ is most easily defined in Fourier space; specifically through multiplication of the Fourier transform $\tilde{F}(q)$ by a factor of $-|q|^\alpha$. Another form of the operator, given in Ref. [25], is

$$\frac{\partial^\alpha}{\partial|x|^\alpha} := -(-\Delta)^{\alpha/2}, \tag{4}$$

where $(-\Delta)$ is the positive definite operator associated with the regular Laplacian, with symbol $|q|^2$. For this reason, $-($

*andrea.zoia@polimi.it

$-\Delta)^{\alpha/2}$ is also called the *fractional Laplacian*. (For $\alpha=2$ we recover the usual Laplacian [17,18].)

Thanks to expression (3), Eqs. (1) and (2) on an infinite or periodic support may be easily solved in the transformed space. However, whenever boundary conditions (BCs) break translational invariance, Fourier transformation is of limited use, and the long-range spatial correlations (inherent to the nonlocal nature of the fractional Laplacian operator) make the problem nontrivial.

In this paper, we investigate the fractional Laplacian on a bounded $1-d$ domain with various BCs on the two sides of the interval. In particular, we shall study absorbing and free BCs: the former naturally arise in the context of Lévy flights in connection to first-passage problems [12,26], while the latter arise in the context of long-ranged elastic interfaces with no constraints at the ends [27]. The remainder of the paper is organized as follows. In Sec. II we recast Eqs. (1) and (2) into the eigenvalue problem for the fractional Laplacian. We then introduce a specific discretization of the fractional Laplacian, and present the main advantages of our choice. In Sec. III we discuss the implementation of free and absorbing BCs by appealing to the examples of Lévy flights and fluctuating interfaces. The numerical results are presented in Sec. IV, with particular emphasis on the behavior of eigenfunctions close to the boundaries. As discussed in Sec. V, some analytical insights into the problem can be achieved by examining certain exactly solvable limits, and by perturbing around them. We end with a concluding Sec. VI, and Appendix A.

II. MATRIX REPRESENTATION OF THE FRACTIONAL LAPLACIAN

Consider Lévy flights in a domain $\Omega \in \mathcal{R}$: by applying the standard method of separation of variables, the concentration $C(x,t)$ in Eq. (1) may be written as

$$C(x,t) = \sum_k \psi_k(x) e^{\lambda_k t} \int_\Omega \psi_k(y) C(y,0) dy, \qquad (5)$$

where $\psi_k(x)$ and λ_k satisfy

$$-(-\Delta)^{\alpha/2} \psi_k(x) = \lambda_k(\alpha) \psi_k(x), \qquad (6)$$

with the appropriate BCs on $\partial\Omega$. Here $-\lambda_k$ also corresponds to the inverse of the time constant with which the associated eigenfunction $\psi_k(x)$ decays in time. Analogously, in the context of stochastic interfaces, the shape $h(x,t)$ may be decomposed into normal modes $h(x,t)=\Sigma_k \tilde{h}_k(t)\psi_k(x)$, where $\psi_k(x)$ satisfy Eq. (6) and $\tilde{h}_k(t)$ are time-dependent coefficients. Substituting this expression for $h(x,t)$ into Eq. (2), the normal modes are decoupled from each other, easing the computation of correlation functions.

For the case of an unbounded domain or periodic BCs, the set of eigenfunctions and the corresponding spectrum of eigenvalues of the operator in Eq. (6) are known explicitly [17,18]. By contrast, analytical study of Eq. (6) with different BCs is awkward and not completely understood: for absorbing BCs it has been proven that the operator $-(-\Delta)^{\alpha/2}$ on

a bounded domain admits a discrete spectrum of eigenfunctions and that the corresponding eigenvalues are all real and negative and can be ordered so that $-\lambda_1 \le -\lambda_2 \le \cdots \le -\lambda_\infty$. However, the exact values of the eigenvalues and the corresponding eigenfunctions are not known and remain an open question (see, e.g., Ref. [28] and references therein). It is nonetheless both possible and interesting to investigate the properties of the fractional Laplacian numerically, and at least two major approaches exist for this purpose.

The first approach consists in implementing the continuum operator in Eq. (6) with a finite-differences scheme. This is the so-called Grünwald-Letnikov scheme, whose construction is directly based on the integral representation of the fractional Laplacian operator [29–31]. Considerable insight into the behavior of solutions to the fractional diffusion equation on unbounded domains is obtained by this method, and it has been shown to be highly accurate. However, due to some technical difficulties, it cannot be straightforwardly extended to take into account BCs [32–34], though it has been shown that it can incorporate an external potential [35]. For numerical purposes, a discussion of the stability and convergence for different versions of the discretized fractional Laplacian operator is provided, e.g., in [36]. Another finite-element approach to discretization of this continuum operator is presented in [37].

The second approach is intrinsically probabilistic in nature and consists in replacing continuous Lévy flights representing $\partial^\alpha/\partial|x|^\alpha$ with discrete hops on a lattice: a transition probability matrix $P_{l,m}$ is constructed, whose elements represent the probability of performing a jump from position l to m. Analogous to Lévy flights, the jump probability has a power-law tail which after normalization reads $P_{l,m}=1/[2\zeta(\alpha+1)|l-m|^{\alpha+1}]$, where $\zeta(\cdot)$ is the Riemann zeta function [26,38]. Within a more general model, this process was first referred to as a Riemann random walk in Ref. [39]. The matrix $D_{l,m}=P_{l,m}-\delta_{l,m}$, is supposed to converge to the representation of the continuum operator when its size goes to infinity. BCs can be taken into account by properly setting the probabilities for jumps leading out of the domain. This approach, however, has some shortcomings. First, the convergence of the discretized matrix to the continuum operator greatly deteriorates as $\alpha \to 2$, i.e., when approaching the regular Laplacian [26,38,40]. Second, it is strictly limited to the range $\alpha \in (0,2]$, due to its probabilistic underpinnings. A probabilistic approach to the solution of the fractional diffusion equation appears also in [41] and references therein, within the framework of underground particle transport in highly heterogeneous materials. In the same references the connections of particle tracking (random walk) methods with the Grünwald-Letnikov scheme are explored.

Our approach is the following. We are interested in representing the action of the operator in terms of a matrix A such that the eigenvalues and eigenvectors of A converge to the eigenvalues and eigenfunctions of the operator when the size M of the matrix goes to infinity. We start with the Fourier representation of the discretized Laplacian, namely, $-2[1-\cos(q)]$ [in line with the sign convention in Eq. (4)], and raise it to the appropriate power, $-\{2[1-\cos(q)]\}^{\alpha/2}$. The elements of the matrix A, representing the fractional Laplacian, are then obtained by inverting the Fourier transform, as

$$A_{l,m} = - \int_0^{2\pi} \frac{dq}{2\pi} e^{iq(l-m)} \{2[1 - \cos(q)]\}^{\alpha/2}. \qquad (7)$$

This is the definition of a *Toeplitz* symmetrical matrix $A_{l,m}[\phi]$ associated with the generator (the so-called *symbol*) $\phi(q) = \{2[1 - \cos(q)]\}^{\alpha/2}$. The generic matrix elements depend only on $n = |l - m|$ and *ad hoc* algorithms exist for calculating the properties of this class of matrix, such as their smallest eigenvalue and the determinant [42–44]. The integral in Eq. (7) may be evaluated explicitly, to give

$$A_{l,m} = A(n) = \frac{\Gamma(-\alpha/2 + n)\Gamma(\alpha + 1)}{\pi \Gamma(1 + \alpha/2 + n)} \sin\left(\frac{\alpha}{2}\pi\right). \qquad (8)$$

In the special cases when $\alpha/2$ is an integer, $A(n) = (-1)^{\alpha - n + 1} C_{\alpha, \alpha/2 + n}$, where $C_{\alpha, \alpha/2 + n}$ are binomial coefficients. We remark that $A(n) = 0$ for $n > \alpha/2$, as the poles of $\Gamma(-\alpha/2 + n)$ are compensated by the zeros of $\sin(\alpha\pi/2)$ in Eq. (8). The off-diagonal elements $A_{l,m \neq l}$ are all positive when $0 < \alpha \leq 2$, but come with different signs when $\alpha > 2$. Thus, for $\alpha \leq 2$, the matrix A can be normalized and interpreted as the transition probabilities for a Lévy flyer with stability index α.

While superficially similar to the implementation of the fractional derivative with Riemann walks [26,39], our approach offers several advantages. (i) It does not suffer from any derivation in convergence as α approaches 2. The discretization in Ref. [26] is in fact quite different from the Laplacian as $\alpha \to 2$. (ii) Our matrix A is easily extended to values of α outside the interval $0 < \alpha \leq 2$. A probabilistic interpretation (of hopping particles) cannot access these intervals as some matrix elements are negative. (iii) Absorbing and free boundary conditions can be implemented for all values of α. The single structure of a matrix then allows for analytical treatments (such as perturbation theory) as described in the following sections.

III. BOUNDARY CONDITIONS FOR THE EIGENVALUE PROBLEM

Due to the nonlocality of the fractional Laplacian, it is not possible to specify the value of the function $\psi_k(x)$ only locally at the boundaries of a finite domain. Doing so leads to erroneous analytical results, in contrast, e.g., with Monte Carlo simulations [45–48]. This also implies that standard techniques such as the method of images are not applicable [12,32]. Subtle distinctions that do not appear in the case of regular random walks need to be introduced, such as between "first-passage" and "first-arrival" times, or between free and reflecting BCs [12,32]. Therefore, a great amount of ingenuity has been employed to solve even apparently simple problems such as Lévy flights constrained to exist on the half axis [49].

The matrix A introduced in the previous section is *a priori* infinite, thus representing the action of the fractional Laplacian operator on an unbounded domain. Within our approach, BCs can be taken into account by modifying the matrix elements related to positions out of the considered domain in a suitable manner, as will be shown in the following. This
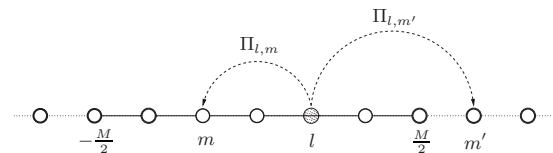

FIG. 1. Implementing BCs in a hopping model: the boundaries of the domain are set at the discrete coordinates $\pm M/2$, i.e., the walk is confined to the interval $-M/2 < l < M/2$. For *absorbing BCs* the jump from l to site m' outside the domain leads to the death of the particle, while for *free BCs* the jump (l, m') is rejected. For both cases, the jump (l, m) within the interval is accepted.

modification leads in general to a matrix of finite size $M + 1$. We will study three different kinds of BCs: absorbing on both sides, free on both sides, and mixed (absorbing on the left and free on the right), with reference to two physical models. The first concerns hopping particles, the second elastic springs; both are well defined for $\alpha \leq 2$ and absorbing, free, and mixed BCs are easily implemented. In principle, the set of rules by which we will take into account BCs can be extended to an arbitrary α.

A. Hopping particles

Let us consider a particle jumping on a one-dimensional discrete lattice, as shown in Fig. 1. When the lattice is infinite, at each time the particle jumps from position l to position $m = l + n$ ($n \neq 0$) with a probability $\Pi_{l,m} = -A(n)/A(0)$. For $\alpha \leq 2$ the probability is well defined if we set $\Pi_{l,l} = 0$, as the elements $A_{l \neq m}$ all have the same sign. This model is naturally connected to Lévy flights, since as shown before A represents the discrete version of the generator of this stochastic process. Let us now discuss how to take into account different BCs on an interval $[-M/2, M/2]$.

Absorbing BCs are imposed by removing the particle whenever a jump takes it to a site m outside the interval. In the special case of Brownian particles, BCs may be assigned locally, since their jumps are of the kind $l \to l \pm 1$ and they must touch the sites $\pm M/2$ in order to leave the interval [2,12,32]. Within our approach, absorbing BCs are implemented by cutting the infinite matrix Π into a matrix of size $(M+1) \times (M+1)$, thus setting to zero all the other elements.

Free BCs are implemented as in the Metropolis Monte Carlo approach: if the sampled m lies outside the allowed interval, then the particle is left at its original location l. This means that the element $\Pi_{l,l}$ is the probability of staying at l. From normalization, clearly we must have $\Pi_{l,l} = 1 - \sum_{l \neq m} \Pi_{l,m}$. These BCs differ from standard reflecting BCs as implemented, e.g., in Refs. [15,34], where particles abandoning the interval are sent to their mirror images with respect to the boundary. Free and reflecting BCs are identical for Brownian particles, thanks to the locality of jumps.

In the case of mixed BCs the particle is removed whenever $m < -M/2$, and remains at l for $m > M/2$. The diagonal element of the matrix thus becomes $\Pi_{l,l} = 1/2 - \sum_{m = l+1}^{M/2} \Pi_{l,m}$.

B. Elastic springs

Now consider a network of springs connecting the sites of a one-dimensional lattice, as shown in Fig. 2. If the spring
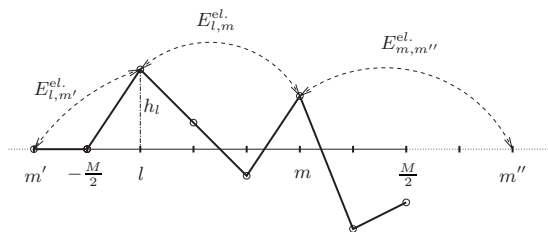
FIG. 2. Implementing BCs in a model of elastic springs: *Mixed BCs* are imposed by removing all springs connected to sites with index $m'' > M/2$ (*absorbing BCs* on the right), and by pinning to zero all sites with index $m' < -M/2$ (*free BCs* on the left). For the case shown here, $E_{l,m}^{el.} = (1/2)A_{l,m}(h_l - h_m)^2$; $E_{l,m'}^{el.} = (1/2)A_{l,m'}h_l^2$; and $E_{m,m''}^{el.} = 0$. The interface is free to fluctuate at the right boundary and is constrained to zero at the left boundary.

constant between sites l and m is $A_{l,m}$, the associated elastic energy is

$$E^{el} = \sum_{l,m} E_{l,m}^{el} = \sum_{l,m} \frac{1}{2} A_{l,m}(h_l - h_m)^2, \qquad (9)$$

where h_l is the displacement of site l. The elastic force acting on the point (l, h_l) is

$$F(h_l) = -\frac{\delta E}{\delta h_l} = -\sum_{l \neq m} A_{l,m}(h_l - h_m). \qquad (10)$$

Such a model also describes the dynamic interfaces with long-range elastic interactions. Let us now discuss how to take into account different BCs on a bounded interval $[-M/2, M/2]$.

Absorbing BCs are implemented in this case by setting $h_m = 0$ outside the interval $[-M/2, M/2]$, thus cutting the infinite matrix A into a matrix of size $(M+1) \times (M+1)$. The diagonal elements are now the same as those of the infinite matrix. Physically, this corresponds to fluctuating interfaces pinned to a flat state outside a domain.

Free BCs are implemented by removing all the springs connecting sites inside the interval to sites outside. The diagonal elements of the matrix are then $A_{l,l} = -\sum_{l \neq m} A_{l,m}$. These conditions allow us to describe fluctuating interfaces with no constraints at the ends: in the past, these BCs have been implemented by using reflecting BCs [20,50,51]. We think that our procedure better represents the physical situation.

For mixed BCs we set $h_m = 0$ for $m < -M/2$, and cut all the springs connecting l with $m > M/2$. The diagonal elements of the matrix become $A_{l,l} = A(0)/2 - \sum_{m=l+1}^{M/2} A_{l,m}$.

IV. NUMERICAL RESULTS

In this section we discuss our numerical results, as obtained by exploiting the above methods. We will mainly focus on the behavior of the first (nontrivial) eigenfunction of Eq. (6), which can be regarded as the dominant mode, and of its associated eigenvalue, which represents the inverse of the slowest time constant. For simplicity, in the following we will assume that $\Omega = [-1, 1]$. Given the matrix A, which now
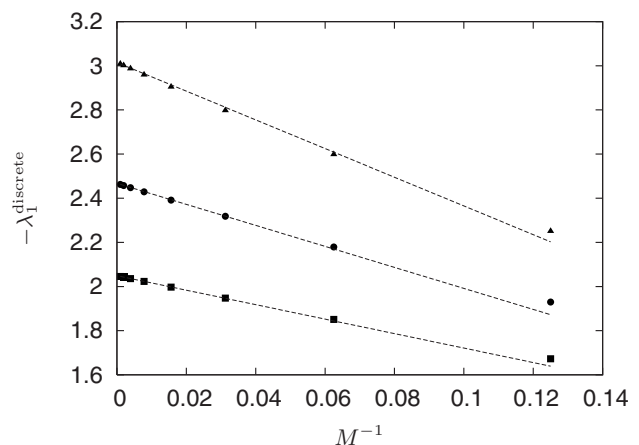

FIG. 3. *Absorbing BCs:* Convergence of the first eigenvalue with M for $\alpha = 1.8$ (squares), 2 (circles), and 2.2 (triangles). Dashed lines are least-squares fits to straight lines, and the continuum limit $\lambda_1(\alpha)$ is obtained for $M^{-1} \to 0$.

is modified so as to incorporate the appropriate BCs, standard numerical algorithms for symmetrical matrices are applied in order to extract the spectrum of eigenvalues and eigenvectors. The accuracy and stability of the proposed method depends on the adopted numerical algorithm: for specific results concerning Toeplitz matrices, we refer the reader to, e.g., [42–44] and references therein. Then, to obtain the continuum limit, the eigenvalues of A are multiplied by a scale factor $\lambda \to \lambda (M/L)^\alpha$, where $L = 2$ is the size of the interval. We remark that, since the first eigenvalue for free BCs is rigorously zero, we focus on the first nontrivial eigenvalue. The eigenvectors of A are naturally defined only up to a multiplicative factor, and the normalization will be specified later.

Let us first discuss the finite-size effects. Numerical evidence shows that in the case of absorbing BCs the eigenvalues of A converge to the continuum limit $\lambda_k(\alpha)$ as M^{-1}. The finite-size exponent appears to be exactly -1, independent of α, while the overall coefficient increases with α. These results are depicted in Fig. 3 for the first eigenvalue: the continuum limit is obtained by extrapolating the least-squares fit of the convergence plot with $M \to \infty$. As opposed to Ref. [26], our method can be extended to any value of α and does not suffer from any slowing down in convergence as $\alpha \to 2$. The extrapolated value for $\alpha = 2$ is $\lambda = -2.467\ldots$, extremely close to the expected value of $-\pi^2/4$.

Finite-size effects are very similar for mixed BCs, while for free BCs the power-law convergence for the first nontrivial eigenvalue has an exponent of -2 and the slope seems to be approximately constant, independent of α.

To explore the structure of the eigenvalues of A for large M, i.e., in the continuum limit, let us define

$$\Lambda_k(\alpha) = [-\lambda_k(\alpha)]^{1/\alpha}. \qquad (11)$$

In Fig. 4 we plot the behavior of $\Lambda_k(\alpha)$ as a function of α for absorbing, free, and mixed BCs. Note that the eigenvalues of the absorbing BC problem exhibit quite monotonic behavior and actually seem to lie on a straight line: we will come back
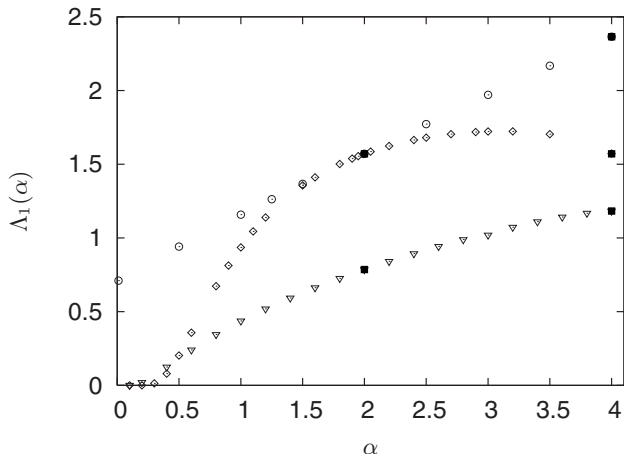
FIG. 4. Eigenvalues with absorbing (circles), free (diamonds), and mixed (triangles) BCs as a function of α. Black squares mark the exact values at $\alpha=2$ and 4 (see Sec. V A).
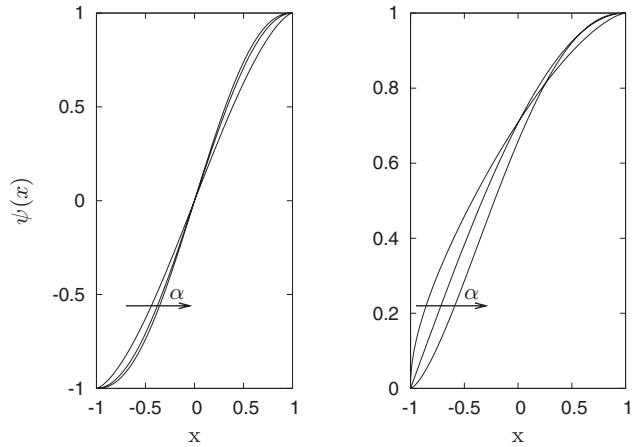

FIG. 6. Eigenfunctions associated with the smallest nontrivial eigenvalue for $\alpha=1$, 2, 3, for free (left) and mixed (right) BCs. The arrow indicates the change in shape of the eigenfunctions for progressively increasing α.

to this point in Sec. V A. Moreover, the eigenvalues of free BCs seem to be tangent to those of absorbing BCs close to the point $\alpha=2$.

In Fig. 5 we illustrate the shapes of the ground-state eigenfunctions of absorbing BCs, corresponding to the first eigenvalue, for different values of α. The eigenfunctions have been normalized such that $\int \psi_1^2(x)dx=1$. A small and a large value of α have been included to emphasize the limiting behavior at the two extremes: for $\alpha \to 0$ the eigenfunction seems to converge to the marker function, while for $\alpha \to \infty$ to a δ function. It can be shown that the latter limit is approached so that [43]

$$\psi_1(x) \sim \frac{\Gamma(3/2+\alpha)}{\sqrt{\pi}\Gamma(1+\alpha)}(1-x^2)^{\alpha/2} \quad \text{as} \ \alpha \to \infty. \quad (12)$$

Typical eigenfunctions for free and mixed BCs are depicted in Fig. 6. In this case the eigenfunctions have been normalized so that their heights range, respectively, in $[-1, \ 1]$ and $[0, 1]$.

An important question is how eigenfunctions behave close to the boundaries. As a specific case, we focused on the case $\alpha=1$, and for absorbing BCs our numerical results indicate $\psi_1(x) \sim (1-|x|)^{1/2}$ as $x \to \pm1$ (see Fig. 7). This result is consistent with the findings of Refs. [38,49], which show
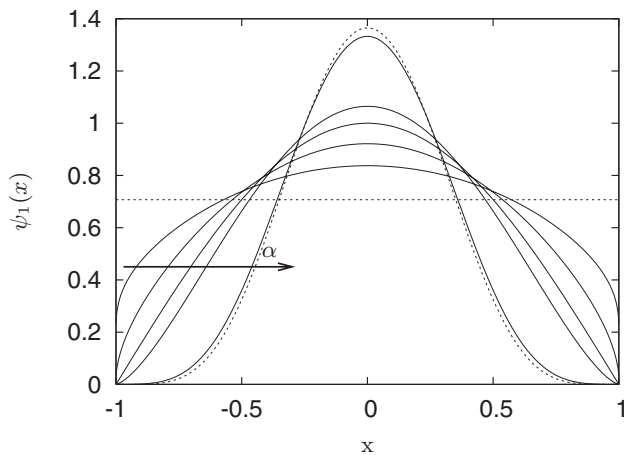

FIG. 5. Eigenfunctions with the smallest eigenvalue λ_1 for $\alpha=0.1$, 2, 3, and 10 for absorbing BCs (the arrow indicates the change in shape of the eigenfunctions for progressively increasing α). The horizontal dashed line corresponds to the limiting function for $\alpha \to 0$ (marker function). For comparison, we also show the asymptotic form of Eq. (12) for $\alpha=10$ as a dotted line.
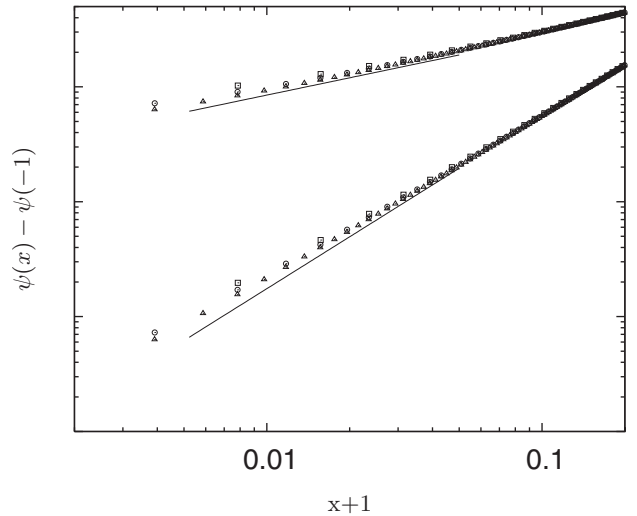

FIG. 7. Scaling of the first eigenfunction close to the boundary for fractional Laplacian of $\alpha=1$, with absorbing (top) and free (bottom) BCs. Symbols correspond to numerical eigenvectors for $M=256$ (squares), 512 (circles), and 1024 (triangles), while solid lines correspond to $(x+1)^{1/2}$ and $(x+1)^{3/2}$, respectively. The y axis is in arbitrary units (logarithmic scale).

that in general for absorbing BCs the eigenfunctions scale as $(-|x|+1)^{\alpha/2}$. The limiting behavior for free BCs in Fig. 7 is less clear: the convergence is rather poor, and we are unable to fully characterize the dependence of the slope on α. Nonetheless, we can exclude the simplest ansatz that the eigenfunction for a generic α scales linearly close to the boundaries, as suggested by the behavior at $\alpha=2$ and 0, where $\psi_1(x) \sim (1-|x|)^1$. In fact, the fit in Fig. 7 is for an exponent $\alpha/2+1=3/2$.

V. ANALYTICAL RESULTS FOR ABSORBING BOUNDARY CONDITIONS

For the case of absorbing BCs it is possible to derive further information on the structure of the eigenvalues of Eq. (6) by resorting to an analytical treatment.

A. Even α, and general structure of the eigenvalues

When α is an even integer, the eigenvalue-eigenfunction Eq. (6) may be cast in a different way. In particular, Eq. (3) can be extended to complex q by omitting the absolute value. Then, since $\lambda=-q^\alpha$ is real and negative, we can associate with each λ_k, α independent solutions characterized by $q_j = \Lambda_k \omega_j$, for $j=0,1,\ldots,\alpha-1$, where $\omega_j=\cos(2\pi j/\alpha) + i\sin(2\pi j/\alpha)$ are the αth roots of unity. The general form of an eigenfunction is

$$\psi_k(x) = \sum_{j=0}^{\alpha-1} c_{j,k} e^{i\Lambda_k \omega_j x}, \qquad (13)$$

where $c_{j,k}$ are to be determined by imposing the BCs

$$\psi_k(\pm 1) = \psi_k^{(1)}(\pm 1) = \psi_k^{(\alpha/2-1)}(\pm 1) = 0. \qquad (14)$$

Thus, determining Λ_k is equivalent to finding the zeros of the determinant of the $\alpha \times \alpha$ matrix B,

$$B = \begin{pmatrix} e^{i\Lambda\omega_0} & \cdots & e^{i\Lambda\omega_{\alpha-1}} \\ e^{-i\Lambda\omega_0} & \cdots & e^{-i\Lambda\omega_{\alpha-1}} \\ \vdots & & \vdots \\ \omega_0^{\alpha/2-1}e^{i\Lambda\omega_0} & \cdots & \omega_{\alpha-1}^{\alpha/2-1}e^{i\Lambda\omega_{\alpha-1}} \\ \omega_0^{\alpha/2-1}e^{-i\Lambda\omega_0} & \cdots & \omega_{\alpha-1}^{\alpha/2-1}e^{-i\Lambda\omega_{\alpha-1}} \end{pmatrix}. \qquad (15)$$

The structure of the function $\det(B)=0$ is rather involved. However, for large k it is possible to rewrite this equation in the form

$$f_\alpha(\Lambda_k)\cos(2\Lambda_k) + g_\alpha(\Lambda_k) = 0 \qquad (16)$$

when $\alpha/2$ is even and

$$f_\alpha(\Lambda_k)\sin(2\Lambda_k) + g_\alpha(\Lambda_k) = 0 \qquad (17)$$

when $\alpha/2$ is odd. Here, $f_\alpha(\Lambda_k)=\cosh[2\cot(\pi/\alpha)\Lambda_k]$ and

$$\frac{g_\alpha(\Lambda_k)}{f_\alpha(\Lambda_k)} \sim e^{-2\sin(2\pi/\alpha)\Lambda_k}, \qquad (18)$$

when $k \to \infty$.

Two special cases need to be considered separately: for $\alpha=2$ we have $g_2(\Lambda_k)=0$ and for $\alpha=6$ a fortuitous factoriza-
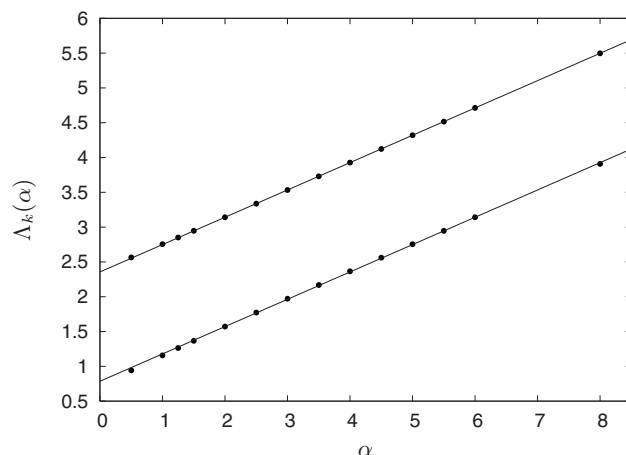

FIG. 8. Λ_k as a function of α for $k=1$ and 2 (dots), compared to the approximation in Eq. (19) (straight lines).

tion gives $g_6(\Lambda_k)=\sin(\Lambda_k)[\cosh(\sqrt{3}\Lambda_k)+\cdots]$. This allows one to conclude that for large k the roots of $\det(B)=0$ converge exponentially fast to those of $\cos(2\Lambda_k)=0$ when $\alpha/2$ is even, or $\sin(2\Lambda_k)=0$ when $\alpha/2$ is odd. These asymptotic roots are exact for $\alpha=2$ for every k and for $\alpha=6$ for all odd k, thanks to the factorization.

These considerations, together with the fact that $\Lambda_k(\alpha) < \Lambda_k(\alpha+2)$, allow us to state that, for fixed α and large k the eigenvalues $\Lambda_k(\alpha)$ will be asymptotically described by a monotonically increasing function whose simplest form is the straight line

$$\Lambda_k^{\mathrm{approx}}(\alpha) = \frac{\pi}{8}\alpha + \frac{\pi}{4}(2k-1). \qquad (19)$$

Equation (19) is consistent with our numerical findings and generalizes an observation by Rayleigh that for $\alpha=4$ the two values $\Lambda_k(\alpha)$ and $\Lambda_k^{\mathrm{approx}}(\alpha)$ are identical to the sixth decimal digit for $k \geq 4$ [52]. In particular, we remark that direct numerical evaluation of $\det(B)=0$ reveals that Eq. (19) is a very good approximation even for $k=1$ if α is not too large, while it has been shown that for very large α the asymptotic behavior of the first eigenvalue is [43]

$$\Lambda_1(\alpha) = (4\alpha\pi)^{1/2\alpha}\frac{\alpha}{e}. \qquad (20)$$

Surprisingly, the asymptotic form of Eq. (19) is valid also for a generic real α, as shown in Fig. 8 for $k=1$ and 2. Setting aside some special cases of α such as 2 and 4, to our best knowledge the approximation in Eq. (19) is a new result. To illustrate the trends, the error in the approximation in depicted in Fig. 9. In all cases considered, numerical results indicate that the error vanishes exponentially for large k, in agreement with the analytical findings for even α.

B. Perturbation theory

We next examine the behavior of eigenvalues close to $\alpha=2$ and 0 using standard perturbation theory. Throughout
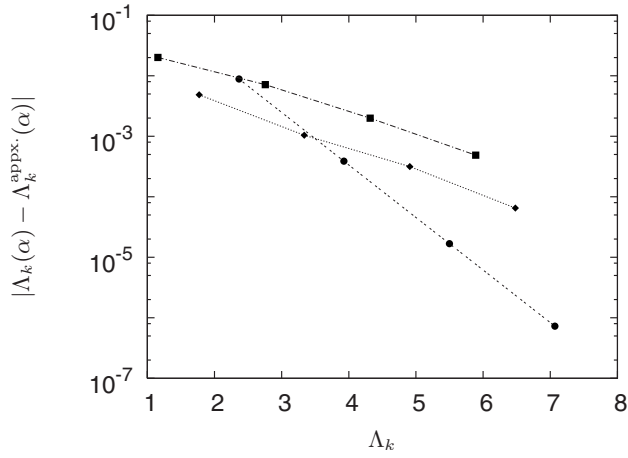
FIG. 9. The difference between $\Lambda_k(\alpha)$ and $\Lambda_k^{\text{approx}}(\alpha)$ for $\alpha=1$ (squares), 2.5 (diamonds), and 4 (dots), as a function of Λ_k.

this section we will consider a symmetric domain $\Omega=[-L/2,L/2]$.

1. Perturbation around $\alpha=2$

The ground state eigenvector for $\alpha=2$ on the discrete interval $[-M/2,M/2]$ is

$$\psi_1(l) = \sqrt{\frac{2}{M}}\cos\left(\frac{\pi l}{M}\right), \qquad (21)$$

with a corresponding eigenvalue of

$$\lambda_1 = \left(\frac{M}{L}\right)^\alpha \langle\psi_1|A|\psi_1\rangle, \qquad (22)$$

where L is the length of the interval. In order to deal with dimensionless quantities, we multiply λ_1 by L^α, and set

$$\hat{\lambda}_1 = \lambda_1 L^\alpha = M^\alpha\langle\psi_1|A|\psi_1\rangle. \qquad (23)$$

For $\alpha=2$, where $A(0)=-2$, $A(1)=1$, and $A(n>1)=0$, we have

$$\hat{\lambda}_1 = -M^2\left[2 - 2\cos\left(\frac{\pi}{M}\right)\right] \sim -\pi^2. \qquad (24)$$

Setting $\alpha=2+\epsilon$, the operator $A(n)$ becomes, at first order in ϵ:

$$A(n) = \begin{cases} -2-\epsilon & \text{for } n=0, \\[2mm] 1+\dfrac{3}{4}\epsilon & \text{for } n=1, \\[2mm] -\dfrac{1}{(n+1)n(n-1)}\epsilon & \text{for } n>1. \end{cases} \qquad (25)$$

The correction to the ground state is given by

$$\hat{\lambda}_1^* = \hat{\lambda}_1 + \delta\hat{\lambda} = M^{2+\epsilon}\langle\psi_1|A|\psi_1\rangle, \qquad (26)$$

which can be rewritten in the following way:

$$\frac{\hat{\lambda}_1^*}{M^{2+\epsilon}} = A(0) + 2\sum_{n=1}^M A(n)\sum_{l=-M/2}^{M/2-n}\psi_1(l)\psi_1(l+n).$$

By noticing that

$$\sum_{l=-M/2}^{M/2-n}\psi_1(l)\psi_1(l+n) = \frac{M-n}{M}\cos\left(\frac{n\pi}{M}\right) + \frac{1}{\pi}\sin\left(\frac{n\pi}{M}\right),$$

we can rewrite the previous expression as

$$\hat{\lambda}_1^* = -M^{2+\epsilon}\left(\frac{\pi^2}{M^2} + \epsilon Q\right),$$

where Q, in the limit of large M, is given by

$$Q = -\frac{1}{2} + \frac{3}{4}\frac{\pi^2}{M^2} + 2\sum_{n=2}^M A(n)\left(1 - \frac{1}{2}\frac{n^2\pi^2}{M^2}\right)$$
$$+ \frac{2}{M^2}\int_0^1 dx\,\frac{(1-x)\cos(\pi x) + [\sin(\pi x)]/\pi - 1 + \pi^2x^2/2}{x^3}.$$

Performing the integration, we find

$$QM^2 = -\pi^2\ln(M) + \pi[\text{Si}(\pi) + \pi\ln(\pi) - \pi\text{Ci}(\pi)],$$

where Si and Ci are the integral sine and integral cosine functions, respectively [53]. We can finally come back to λ_1^*, which, expanding for small ϵ, reads

$$\hat{\lambda}_1^* = -\pi^2 + \epsilon[\pi^2\text{Ci}(\pi) - \pi\text{Si}(\pi) - \pi^2\ln(\pi)]. \qquad (27)$$

This approach can be extended to eigenfunctions $\psi_k(l)$ of every order k. By replacing $\psi_1(l)$ in Eq. (26) with the generic $\psi_k(l)$ (see Appendix A 2) and performing the summations as shown above, after some algebra we find the first-order correction $\delta\hat{\lambda}_k = \hat{\lambda}_k^* - \hat{\lambda}_k$, with

$$\delta\hat{\lambda}_k = \epsilon[k^2\pi^2\text{Ci}(k\pi) - k\pi\text{Si}(k\pi) - k^2\pi^2\ln(k\pi)]. \qquad (28)$$

Now, consider the curve $\lambda_k^{\text{approx}}$, which after rescaling by a factor L^α gives

$$\hat{\lambda}_k^{\text{approx}} = -\left(\frac{\pi}{4}\alpha + \frac{\pi}{2}(2k-1)\right)^\alpha. \qquad (29)$$

By putting $\alpha\to2+\epsilon$ and expanding for small ϵ, we get

$$\delta\hat{\lambda}_k^{\text{approx}} = \epsilon\left(-k\frac{\pi^2}{2} - k^2\pi^2\ln(k\pi)\right). \qquad (30)$$

We can thus compare Eq. (28), which derives from the perturbative calculations, with Eq. (30), which stems from our generic approximation to the eigenvalues of Eq. (6). In Fig. 10 we plot the error $\delta\hat{\lambda}_k - \delta\hat{\lambda}_k^{\text{approx}}$ as a function of $k\pi$. As k increases, the slope of the curve along which the actual eigenvalues lie in the proximity of $\alpha=2$ approaches very rapidly the slope of the curve $\hat{\lambda}_k^{\text{approx}}$.

We have also applied perturbation theory for $\alpha=2$ to the case of free BCs, for which the eigenfunctions are known analytically (see Appendix A 2). Calculations analogous to those leading to Eq. (28) allow us to derive $\delta\hat{\lambda}_k$ as

$$\delta\hat{\lambda}_k = \epsilon[4 + k^2\pi^2\mathrm{Ci}(k\pi) - 3k\pi\,\mathrm{Si}(k\pi) - k^2\pi^2\ln(k\pi)$$
$$+ 2k\pi\,\mathrm{Si}(2k\pi)]. \tag{31}$$

The values of $\delta\hat{\lambda}_k$ for free BCs are close but not equal to those of absorbing BCs, thus ruling out the hypothesis that the curves $\Lambda_k(\alpha)$ for free and absorbing BCs are tangent near the point $\alpha=2$.

2. Perturbation around $\alpha=0$

When α is 0, $\partial^0/\partial|x|^0$ becomes the identity operator $-I$ and the associated first (and only) eigenvalue is $\lambda_1(\alpha)=1$. In principle, for $\alpha=0$ the operator is highly degenerate, but considering the limiting behavior and the scaling behavior near the boundaries we are led to conclude that the discrete ground state eigenvector for $\alpha=0$ is

$$\psi_1(l) = \frac{1}{\sqrt{M+1}}I_\Omega(l), \tag{32}$$

where $I_\Omega(l)$ is the marker function of the domain $\Omega=[-M/2,M/2]$ (see Fig. 5). Setting $\alpha=0+\epsilon$, the operator $A(n)$ is corrected at the first order as

$$A(n) = \begin{cases} -1 + o(\epsilon^2) & \text{for } n=0, \\ \dfrac{1}{2n}\epsilon & \text{for } n>0. \end{cases} \tag{33}$$

The correction to the ground state is given by

$$\hat{\lambda}_1^* = \frac{M^\epsilon}{M+1}\sum_{l,m}I_\Omega(l)A(n)I_\Omega(m), \tag{34}$$

which in the limit of large M is

$$\hat{\lambda}_1^* = -M^\epsilon[1 - \epsilon\ln(M) + \epsilon(1-\gamma)], \tag{35}$$

where $\gamma=0.577\,215\,66\ldots$ is the Euler-Mascheroni constant. Expanding for small ϵ, we finally get

$$\hat{\lambda}_1^* = -1 - \epsilon(1-\gamma). \tag{36}$$

This value is to be compared with $\hat{\lambda}^{\mathrm{approx}}$, which for $\alpha=0+\epsilon$ reads

$$\hat{\lambda}_1^{\mathrm{approx}} = -1 - \epsilon\ln\left(\frac{\pi}{2}\right). \tag{37}$$

C. First-passage-time distribution

Knowledge of the fractional Laplacian operator allows us to address the temporal behavior of the Lévy flyer concentration $C(x,t|x_0)$, where x_0 is the starting position of walkers at $t=0$. For example, let us consider the first-passage-time distribution for the one-dimensional bounded domain Ω with absorbing BCs on both sides, which is obtained as [54]

$$\rho(t|x_0) = -\frac{\partial}{\partial t}\int_\Omega dx\, C(x,t|x_0). \tag{38}$$

In particular, moments of the distribution $\rho(t|x_0)$ are given by

$$\langle t^m\rangle(x_0) = \int_0^\infty dt\, t^m\rho(t|x_0) = -\int_0^\infty dt\, t^m\frac{\partial}{\partial t}\int_\Omega C(x,t|x_0). \tag{39}$$

For $m=1$, integrating by parts and using the relation

$$\frac{\partial}{\partial t}C(x,t|x_0) = \frac{\partial^\alpha}{\partial|x_0|^\alpha}C(x,t|x_0), \tag{40}$$

we get

$$\frac{\partial^\alpha}{\partial|x_0|^\alpha}\langle t^1\rangle(x_0) = \int_\Omega dx\, C(x,\infty|x_0) - \int_\Omega dx\, C(x,0|x_0) = -1. \tag{41}$$

This equation for the mean first-passage-time (MFPT) may be solved analytically in closed form (see Ref. [38] and references therein), to give $\langle t^1\rangle(x_0)=[(L/2)^2-x_0^2]^{\alpha/2}/\Gamma(\alpha+1)$, where L is the length of the bounded interval (we have assumed that the interval is symmetric around the origin $x=0$). In Fig. 11 we compare this expression with the numerical solution obtained by replacing the fractional Laplacian with the discrete operator A, namely, $\langle t^1\rangle(x_0)=-A^{-1}1(L/M)^\alpha$; the two curves are in excellent agreement for all α and x_0. We remark that the required inversion of the discrete operator may be efficiently performed thanks to the fact that A is a Toeplitz matrix [44].

Analogous calculations for the second moment $m=2$ lead to

$$\frac{\partial^\alpha}{\partial|x_0|^\alpha}\langle t^2\rangle(x_0) = -2\langle t^1\rangle(x_0). \tag{42}$$

More generally, the moments of the first-passage-time distribution are obtained recursively from

$$\frac{\partial^\alpha}{\partial|x_0|^\alpha}\langle t^m\rangle(x_0) = -m\langle t^{m-1}\rangle(x_0), \tag{43}$$

for $m=1,2,\ldots$.

This expression can be rewritten as

$$\left(\frac{\partial^\alpha}{\partial|x_0|^\alpha}\right)^m\langle t^m\rangle(x_0) = (-1)^m\Gamma(m+1). \tag{44}$$

Solving this relation numerically, namely, $\langle t^m\rangle(x_0)=(-1)^m\Gamma(m+1)(L/M)^{m\alpha}A^{-m}1$, allows us to compute all the moments of the first-passage-time distribution, which is akin to knowing the full distribution.

VI. CONCLUSIONS

In this paper, we have studied the eigenvalue-eigenfunction problem for the fractional Laplacian of order α with absorbing and free BCs on a bounded domain. This problem has applications to many physical systems, including Lévy flights and stochastic interfaces. We have proposed a discretized version of the operator whose properties are better suited to bounded domains. It does not suffer from any slowing down in convergence and can easily take into ac-
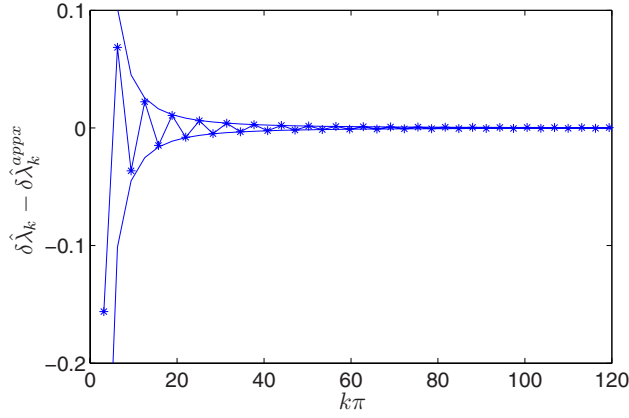
FIG. 10. (Color online) The error in slope of $\delta\hat{\lambda}_k$, compared to Eq. (30) for $\alpha=2$ as a function of $k\pi$ (asterisks). The enveloping dashed curves are $\pm 4/(k\pi)^2$.

count BCs. When $\alpha \leq 2$, the discrete fractional Laplacian may be interpreted in the light of two physical models for hopping particles and for elastic springs, where the BCs emerge naturally and are easily implemented. An analytical continuation for $\alpha > 2$ is also discussed. Our approach easily allows one to obtain the numerical eigenfunctions and eigenvalues for the fractional operator: eigenfunctions corresponding to absorbing BCs show the expected power-law behavior at the boundaries. We also gain analytical insights into the problem by calculating perturbative corrections for the eigenvalues around $\alpha=0$ and 2. Further information on the eigenvalue structure is obtained by studying the case of even α, where a semianalytical treatment is possible: for every α the spectra seem to approach exponentially fast a simple functional form. This conjecture has been proven for the case of even α and is supported by numerical investigations for real α. The first-passage problem and its connection to the fractional Laplacian operator were also explored.

APPENDIX A: ADDITIONAL NOTES

1. Integral representation of Riesz derivatives

Riesz fractional derivatives are defined as a linear combination of left and right Riemann-Liouville derivatives of fractional order, namely,

$$\frac{\partial^\alpha}{\partial |x|^\alpha} f(x) = -\frac{1}{2\cos[(m-\alpha)\pi/2]}[\mathcal{D}_+^\alpha - \mathcal{D}_-^\alpha], \quad (A1)$$

where

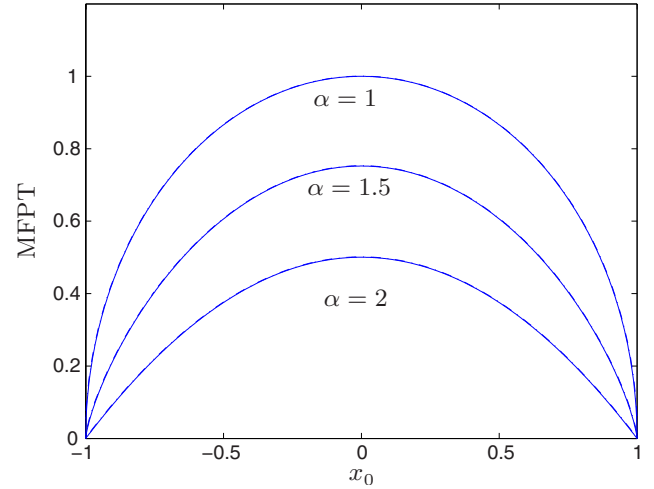$$\mathcal{D}_+^\alpha = \frac{1}{\Gamma(\alpha)} \int_a^x dy(x-y)^{m-\alpha-1} f^{(m)}(y) \quad (A2)$$

and

FIG. 11. (Color online) MFPT as a function of the starting point x_0 for $\alpha=1$, 1.5, and 2. Here $L=2$ and $M=1024$. Solid lines are the analytical result $\langle t^1 \rangle(x_0)=(1-x_0^2)^{\alpha/2}/\Gamma(\alpha+1)$, while dashed lines are obtained from the numerical solution $\langle t^1 \rangle(x_0)=-A^{-1}1(2/M)^\alpha$. In the limit of large M, the two results are in complete agreement for all x_0 and α.

$$\mathcal{D}_-^\alpha = \frac{1}{\Gamma(\alpha)} \int_x^b dy(y-x)^{m-\alpha-1} f^{(m)}(y), \quad (A3)$$

with $\alpha \in (m-1, m)$, m integer, and $x \in \Omega = [a, b]$. This definition does not hold for odd α. The integrals in Eq. (A1) have a power-law decaying kernel [17,18].

2. Eigenfunctions of $-(-\Delta)^{\alpha/2}$ for even α

When $\alpha=2$ the operator in Eq. (6) is the regular Laplacian. For the case of absorbing BCs we impose $\psi_k(-1) = \psi_k(1)=0$ and get

$$\psi_k(x) = \begin{cases} \cos\left(\dfrac{k\pi x}{2}\right) & \text{when } k \text{ is odd}, \\[2ex] \sin\left(\dfrac{k\pi x}{2}\right) & \text{when } k \text{ is even}. \end{cases} \quad (A4)$$

The associated eigenvalues are $\lambda_k=(k\pi/2)^2$, where $k=1,2,\ldots$. For the case of free BCs we impose $\psi_k^{(1)}(-1) = \psi_k^{(1)}(1)=0$ and get

$$\psi_k(x) = \begin{cases} \cos\left(\dfrac{(k-1)\pi x}{2}\right) & \text{when } k \text{ is odd}, \\[2ex] \sin\left(\dfrac{(k-1)\pi x}{2}\right) & \text{when } k \text{ is even}. \end{cases} \quad (A5)$$

The associated eigenvalues are $\lambda_k=[(k-1)\pi/2]^2$, where

$k=1,2,\ldots$. For mixed BCs, namely, $\psi_k(-1)=\psi_k^{(1)}(1)=0$, we have

$$\psi_k(x) = \pm \frac{1}{\sqrt{2}}\left[\cos\left(\frac{(2k-1)\pi x}{4}\right) + (\right.$$
$$\left. -1)^{k+1}\sin\left(\frac{(2k-1)\pi x}{4}\right)\right]. \tag{A6}$$

and the associated eigenvalues are $\lambda_k=[(2k-1)\pi/4]^2$, where $k=1,2,\ldots$.

For absorbing BCs, we present here also the analytical expressions for the eigenfunctions corresponding to the first even values of α. For $\alpha=4$, the condition $\det(B)=0$ becomes $\cos(2\Lambda_k)\cosh(2\Lambda_k)=1$, whose first roots are $\Lambda_1=2.365\,02\ldots$, $\Lambda_2=3.9266\ldots$, and so on. Correspondingly, the normalized eigenfunctions are

$$\psi_k(x) = \begin{cases} \dfrac{\cos(\Lambda_k x)}{\sqrt{2}\,\cos(\Lambda_k)} - \dfrac{\cosh(\Lambda_k x)}{\sqrt{2}\,\cosh(\Lambda_k)} & \text{when } k \text{ is odd,} \\[2ex] \dfrac{\sin(\Lambda_k x)}{\sqrt{2}\,\cos(\Lambda_k)} - \dfrac{\sinh(\Lambda_k x)}{\sqrt{2}\,\cosh(\Lambda_k)} & \text{when } k \text{ is even.} \end{cases} \tag{A7}$$

For the case $\alpha=6$, due to the highly symmetric structure of the determinant equation, the eigenfunctions may be expressed in closed form. For example, the normalized ground state eigenfunction is

$$\psi_1(x) = \tanh\left(\frac{\sqrt{3}\pi}{2}\right)\cos(\pi x)$$
$$+ \frac{\sqrt{3}}{\cosh(\sqrt{3}\pi/2)}\cos\left(\frac{\pi}{2}x\right)\cosh\left(\frac{\sqrt{3}\pi}{2}x\right)$$
$$+ \frac{1}{\cosh(\sqrt{3}\pi/2)}\sin\left(\frac{\pi}{2}x\right)\sinh\left(\frac{\sqrt{3}\pi}{2}x\right). \tag{A8}$$

[1] B. D. Hughes, *Random Walks and Random Environments* (Clarendon Press, Oxford, 1995), Vol. 1.

[2] W. Feller, *An Introduction to Probability Theory and Its Applications*, 3rd ed. (Wiley, New York, 1970), Vol. 1.

[3] R. Metzler and J. Klafter, Phys. Rep. **339**, 1 (2000).

[4] J. Klafter, M. F. Shlesinger, and G. Zumofen, Phys. Today **49** (2), 33 (1996).

[5] R. Metzler and J. Klafter, J. Phys. A **37**, R161 (2004).

[6] P. Lévy, *Théorie de l'Addition des Variables Aléatoires* (Gauthier-Villars, Paris, 1937).

[7] B. V. Gnedenko and A. N. Kolmogorov, *Limit Distributions for Sums of Independent Random Variables* (Addison-Wesley, Reading, MA, 1954).

[8] B. B. Mandelbrot and J. W. van Ness, SIAM Rev. **10**, 422 (1968).

[9] B. B. Mandelbrot and J. W. van Ness, J. Bus. **36**, 394 (1963).

[10] A. N. Kolmogorov, Rep. Acad. Sci. USSR **26**, 6 (1940).

[11] M. F. Shlesinger, G. M. Zaslavsky, and J. Klafter, Nature (London) **363**, 31 (1993).

[12] A. V. Chechkin, V. Yu. Gonchar, J. Klafter, and R. Metzler, Adv. Chem. Phys. **133**, 439 (2006).

[13] *Lévy Flights and Related Topics in Physics: Proceedings of the International Workshop, Nice, France, 1994,* edited by G. M. Zaslavsky, M. F. Shlesinger, and U. Frisch (Springer-Verlag, Berlin, 1994).

[14] G. M. Zaslavsky, *Hamiltonian Chaos and Fractional Dynamics* (Oxford University Press, Oxford, 2005).

[15] A. Mildenberger, A. R. Subramaniam, R. Narayanan, F. Evers, I. A. Gruzberg, and A. D. Mirlin, Phys. Rev. B **75**, 094204 (2007).

[16] A. D. Mirlin and F. Evers, Phys. Rev. B **62**, 7920 (2000).

[17] I. Podlubny, *Fractional Differential Equations* (Academic Press, London, 1999).

[18] S. G. Samko, A. A. Kilbas, and O. I. Maritchev, *Fractional Integrals and Derivatives* (Gordon and Breach, New York, 1993).

[19] S. N. Majumdar and A. J. Bray, Phys. Rev. Lett. **86**, 3700 (2001).

[20] T. Antal, M. Droz, G. Györgyi, and Z. Rácz, Phys. Rev. E **65**, 046140 (2002).

[21] S. F. Edwards and D. R. Wilkinson, Proc. R. Soc. London, Ser. A **381**, 17 (1982).

[22] H. Gao and J. R. Rice, J. Appl. Mech. **65**, 828 (1989).

[23] J. F. Joanny and P. G. de Gennes, J. Chem. Phys. **81**, 552 (1984).

[24] Z. Toroczkai and E. D. Williams, Phys. Today **52** (12), 24 (1999).

[25] A. Saichev and G. M. Zaslavsky, Chaos **7**, 753 (1997).

[26] S. V. Buldyrev, M. Gitterman, S. Havlin, A. Ya. Kazakov, M. G. E. da Luz, E. P. Raposo, H. E. Stanley, and G. M. Viswanathan, Physica A **302**, 148 (2001).

[27] R. Santachiara, A. Rosso, and W. Krauth, J. Stat. Mech.: Theory Exp. (2005) L08001; (2007) P02009.

[28] R. Bañuelos, T. Kulczycki, and J. P. Méndez-Hernández, Potential Anal. **24**, 205 (2006).

[29] R. Gorenflo, F. Mainardi, D. Moretti, G. Pagnini, and P. Paradisi, Chem. Phys. **284**, 521 (2002).

[30] R. Gorenflo, G. De Fabritiis, and F. Mainardi, Physica A **269**, 79 (1999).

[31] R. Gorenflo and F. Mainardi, J. Anal. Appl. **18**, 231 (1999).

[32] A. V. Chechkin, R. Metzler, V. Y. Gonchar, J. Klafter, and L. V. Tanatarov, J. Phys. A **36**, L537 (2003).

[33] M. Ciesielski and J. Leszczynski, J. Theor. Appl. Mech. **44**, 393 (2006).

[34] N. Krepysheva, L. Di Pietro, and M.-C. Néel, Phys. Rev. E **73**, 021104 (2006).

[35] A. V. Chechkin, V. Y. Gonchar, J. Klafter, R. Metzler, and L. V. Tanatarov, J. Stat. Phys. **115**, 1505 (2004).

[36] V. E. Lynch, B. A. Carreras, D. del-Castillo-Negrete, K. M. Ferreira-Mejias, and H. R. Hicks, J. Comput. Phys. **192**, 406

(2003).

[37] W. Chen and S. Holm, J. Acoust. Soc. Am. **115**, 4 (2004).

[38] S. V. Buldyrev, S. Havlin, A. Ya. Kazakov, M. G. E. da Luz, E. P. Raposo, H. E. Stanley, and G. M. Viswanathan, Phys. Rev. E **64**, 041108 (2001).

[39] B. D. Hughes, E. W. Montroll, and M. F. Shlesinger, J. Stat. Phys. **30**, 273 (1983).

[40] M. Marseguerra and A. Zoia, Physica A **377**, 1 (2007).

[41] Z. Yong, D. A. Benson, M. M. Meerschaert, and H.-P. Scheffler, J. Stat. Phys. **123**, 89 (2006).

[42] E. L. Basor and K. E. Morrison, Linear Algebr. Appl. **202**, 129 (1994).

[43] A. Böttcher and H. Widom, Oper. Theor.: Adv. Appl. **171**, 73 (2006).

[44] W. Mackens and H. Voss, SIAM J. Matrix Anal. Appl. **18**, 521 (1997).

[45] B. Dybiec, E. Gudowska-Nowak, and P. Hänggi, Phys. Rev. E **73**, 046104 (2006).

[46] M. Gitterman, Phys. Rev. E **62**, 6065 (2000).

[47] M. Ferraro and L. Zaninetti, Phys. Rev. E **73**, 057102 (2006).

[48] S. L. A. de Queiroz, Phys. Rev. E **71**, 016134 (2005).

[49] G. Zumofen and J. Klafter, Phys. Rev. E **51**, 2805 (1995).

[50] S. Moulinet, A. Rosso, W. Krauth, and E. Rolley, Phys. Rev. E **69**, 035103(R) (2004).

[51] P. Le Doussal and K. J. Wiese, Phys. Rev. E **68**, 046118 (2003).

[52] J. W. S. Rayleigh, *The Theory of Sound* (Dover, New York, 1969).

[53] *Handbook of Mathematical Functions with Formulas, Graphs, and Mathematical Tables*, 9th ed., edited by M. Abramowitz and I. A. Stegun (Dover, New York, 1972), pp. 231–233.

[54] S. Redner, *A Guide to First-Passage Processes* (Cambridge University Press, Cambridge, 2001).